J Mater Sci (2007) 42:8292–8297
DOI 10.1007/s10853-007-1509-x

Preparation and characterization of nanosized bismuth doped tin dioxide powders with a novel post treatment process

Qiuxing He · Weiping Tu · Jianqing Hu

Received: 29 September 2006 / Accepted: 9 January 2007 / Published online: 4 July 2007

Abstract Bismuth-doped tin dioxide (BTO) nanopowders were prepared by wet chemical co-precipitation method using tin tetrachloride ($SnCl_4$) and bismuth nitrate ($Bi(NO_3)_3$) as raw materials. Effects of calcination temperature and post treatment methods on particle size and crystalline phase transition of bismuth tin precursor (BTP) were studied by X-ray diffraction (XRD), transmission electron microscopy (TEM), thermogravimetric-differential scanning calorimetric instrument (TG-DSC) and X-ray photoelectron spectroscopy (XPS). The optimal calcination temperature of BTP was found to be about 873 K. A novel post treatment process with polyacrylamide (PAM) in the preparation of nanometerials was presented for the first time. Experimental results showed that nonionic PAM is a highly effective additive, which not only speeds up the filtration of precursor, but also effectively reduces the formation of hard agglomerates. The average size of BTO nanopowders prepared using nonionic PAM as a filtration aid and disperser is smaller than 10 nm. We believe this post treatment method will come into wide use for preparation of many nanosized materials.

Introduction

Tin dioxide (SnO_2) is a type of high band gap semiconductor material, which is widely applied to solar cells, energy-saving devices, anti-electrostatic films, electromagnetic shielding materials, etc [1, 2]. In the research field of SnO_2 functional material, new spectrum-selectivity nanometer coatings has received much focus recently due to its transparent nature while being a good thermal insulator [3]. Preparation of this nanometer coating involves selecting of nanometer material that has good spectrum selectivity and is easily dispersed into organic coatings without agglomeration [4, 5]. Pure SnO_2 powders have many shortcomings, such as uncontrollable crystal grain dimensions, thermally instable crystal structure and weak spectrum selectivity [6]. Doping is the best way to overcome these defeats [7]. F and Sb doped Tin dioxide has been studied widely [8–11], while bismuth-doped tin dioxide has not been reported yet.

As a kind of electron doped functional materials, Bismuth is extensively applied to gas sensing devices, electrolyte materials, photo-electric materials, high temperature superconductor materials, dielectric ceramics, etc [12, 13]. Bi_2O_3 has a monocline structure, which possesses many oxide vacancy defects and has high electrical conductivity [14]. Nanosized Bi_2O_3 powders have excellent optical nonlinear response.

For the preparation of nanomaterials, many methods were introduced. The method of wet chemical co-precipitation is considered the commonest way for preparing of nanomaterials of metal oxides due to its simple technique, low cost, controllable stoichiometry ratio and use of convenient materials. However, the method has the drawbacks of hard agglomerates and long detachment of precursor, which is becoming a bottleneck to the mass production of nanomaterials.

As a flocculating agent, PAM has been widely applied to the treatment of wastewater, while its use in the preparation of nanomaterials has not been reported yet. In order to

Q. He · W. Tu (✉) · J. Hu
School of Chemical and Energy Engineering, South China University of Technology, Guangzhou 510640, China
e-mail: cewptu@scut.edu.cn

Q. He
College of Pharmacy, Guangdong Pharmaceutical University, Guangzhou 510006, China

shorten the filtration time of precursor and eliminate the formation of hard agglomerates, a novel post treatment method with PAM was presented in this research for the first time. BTO nanomaterials were first prepared by wet chemical co-precipitation using bismuth as a doping agent and PAM as filtration aid and disperser. The preparation process, particle size and phase transition mechanism were also studied.

Experiments

Preparation of BTO nanometer powders

A 300 mL mixture of isopropanol and deionized water ($V/V = 1$) was added into a 500 mL three-necked glass reactor equipped with a Teflon anchor stirrer and a reflux condenser. 10.87 g of $SnCl_4 \cdot 5H_2O$ (analytic reagent), 1.63 g of $Bi(NO_3)_3 \cdot 5H_2O$ (analytic reagent) and 1.0 g polyglycol (analytic reagent, m.W. 1000) were dissolved into the mixture under stirring. An appropriate amount hydrochloric acid (0.5 mol/L) was also added into the solution until clear. The solution was then heated to 343 K, and a calculated amount of aqueous ammonia (3 mol/L) was added dropwise into the solution until the pH was between 7 and 8. Then the solution was allowed to age for 10 min at 343 K.

In order to speed up the solid–liquid solution separation rate and to prevent the aggregation of nanometer particles, a novel post treatment process with polyacrylamide was presented. Three kinds of PAM (cationic PAM, anionic PAM and nonionic PAM) were used as filtration aid in the current research. PAM was added under rapid stirring before the colloidal BTP was filtered under reduced pressure. The PAM concentration used was 0.1% (wt%) with a 5 g dosage.

The resultants treated by PAM were then washed, filtered and dried to obtain bismuth tin precursor (BTP), which were then calcined to produce BTO nanopowders. The doping ratio (X) of Bi is denoted as mol (Bi)/mol (Bi + Sn).

Characterization of BTO nanopowders

(1) The particle morphology and size were studied by transmission electron microscope (TEM, JEM-2010HR/INCA/GATAN CCD). (2) The phase analysis of BTO was carried out by X-ray diffractometer (XRD, XD-3AX) under the following operating conditions: CuKα_1 radiation, voltage 30 kV, current 30 mA, step gap 0.02°, the scan velocity 2°/min, wavelength 0.154 nm. (3) The particle size distribution was measured with a laser particle size apparatus (ZS Nano S, Malvern). (4) The thermo-gravimetric differential scanning calorimetric (TG–DSC) analysis was carried out on the NETZSCH STA 449C. (5) X-ray photoelectron spectroscopy (XPS, Axis ultra DCD, Kratos Corp.) was adopted to determine the specific forms of nano-BTO powder.

Results and discussions

The determination of calcination temperature of BTP

TG–DSC curve of BTP with X = 0.1 is shown in Fig. 1. It can be seen from the TG curve that the total mass loss reaches about 23.5% when BTP is calcined at 773 K. The mass remains constant when the calcination temperature is increased beyond 773 K. This indicated that the crystallization water has been dried out, and that BTP has been transformed into oxide completely. In addition, Bi ionic and Sn ionic and aqueous ammonia occur reaction to form weakly alkaline $Sn(OH)_4$–$Bi(OH)_3$, which was also regarded as another form of $SnO_2 \cdot 2H_2O$–$Bi_2O_3 \cdot 3H_2O$. So, a conclusion could be drawn that BTP really is a complex of an oxide and its crystal hydrate. Correspondingly, the composite molecular formula of BTP can be deduced as $SnO_2 \cdot 2H_2O$–$Bi_2O_3 \cdot 3H_2O$.

As can be seen from the TG–DSC curve, BTP has a strong endothermic peak at 373 K, and about 80% crystallization water was lost at 573 K. At 873 K, there is a relative strong endothermic peak from the DSC curve; however, the TG curve does not change. This indicates that a phase transition occurs at this temperature. In order to explain exactly its phase change, XPS (Fig. 2) shows that there is x = 7% bismuth ionic of nano-BTO, and XRD cannot find a new phase except for SnO_2 although the scan velocity was set from 10°/min to 2°/min. So we think Bi

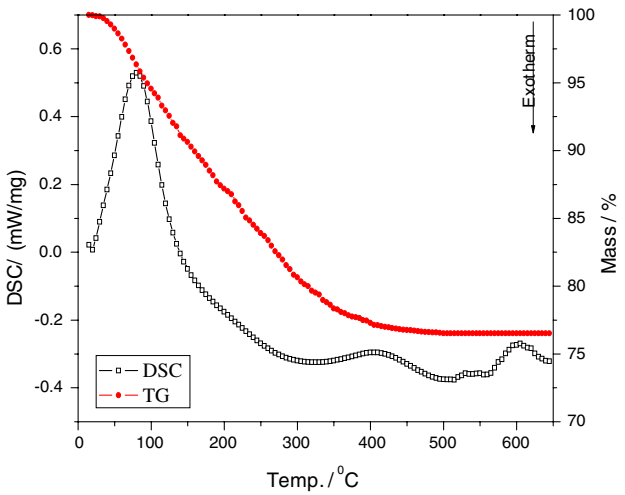

Fig. 1 TG–DSC curves of BTP

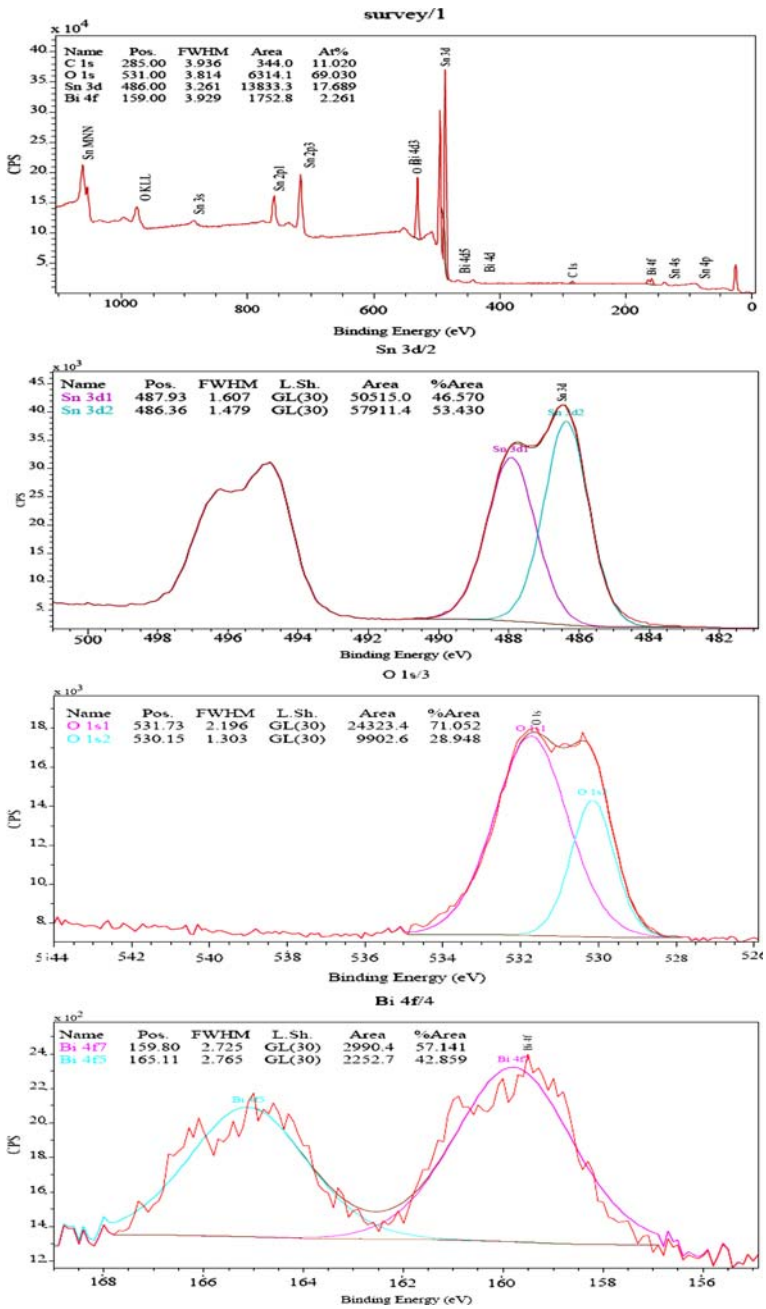

Fig. 2 X-ray photoelectron spectroscopy of nano-BTO

ions enter Sn-vacancies and Bi:SnO_2 is formed. The temperature dependent phase transition process of BTP can be described by the following formula:

$$SnO_2 \cdot 2H_2O - Bi_2O_3 \cdot 3H_2O \overset{300-573\ K}{\longrightarrow}$$

$$SnO_2 \cdot 0.4H_2O - Bi_2O_3 \times 0.6H_2O \overset{673\ K}{\longrightarrow}$$

$$SnO_2 - Bi_2O_3 \underset{Bi}{\overset{873\ K}{\longrightarrow}} xSn_{(1-x)}O_2$$

The XRD pattern of BTO calcined at 873 K with X = 0.1 is displayed in Fig. 3. The diffraction pattern agrees well with a single tetragonal phase of SnO_2 (JCPDS 77-0452). Also there are no diffraction peaks for Bi_2O_3. Therefore, the XRD studies verify the deduction (formula 1). BTP is a crystal hydrate of complex oxides, and the optimal calcination temperature for BTO preparation is 873 K.

Effect of calcination temperature on phase transition and distribution of size

The XRD and TEM of BTO with X = 0.1 prepared at different calcination temperatures are shown in Figs. 3

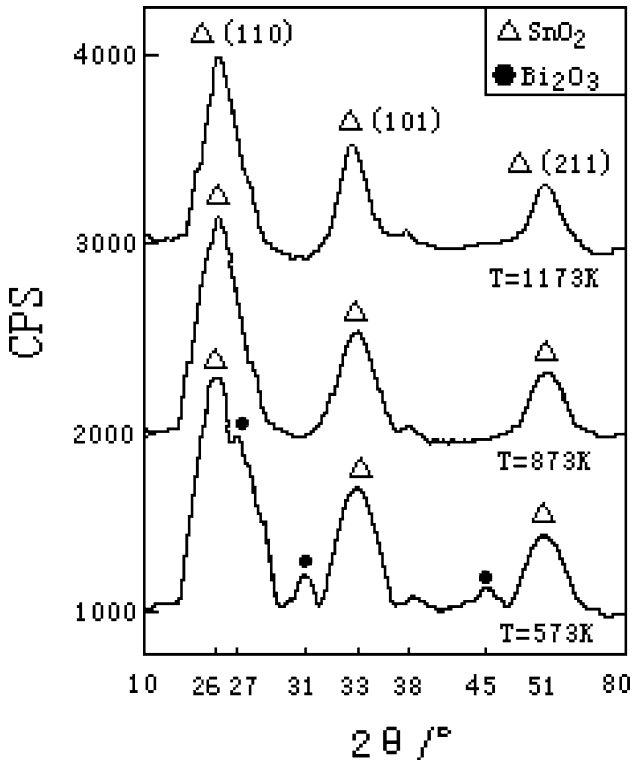

Fig. 3 XRD patterns of BTO powders prepared at different calcination temperature

and 4, respectively. The crystal size can be calculated according to the Debye-Scherr formula $d = \frac{k\lambda}{\beta \cos\theta}$, where $k = 0.89$, $\lambda = 0.15406$ nm, β represents the width of a half peak (unit, radian), and θ is the half diffraction angle. For BTO prepared at 873 K, the crystal size of three specific diffraction peak of (110), (101) and (211) is 5.5 nm, 6.4 nm and 6.5 nm, respectively, with a mean crystal size of 5.8 nm. The dimensions of BTO can also be verified by the TEM photograph shown in Fig. 4(A). The apparent diffraction peaks of SnO_2 and weak diffraction peaks of Bi_2O_3 can be found in XRD of BTO obtained when calcined at 573 K, Which indicates that a mixture of SnO_2–Bi_2O_3 forms when BTP is calcined at the temperature lower than 573 K. The intensity of Bi_2O_3 diffraction peaks decreases with increasing calcination temperature. The Bi_2O_3 diffraction peaks vanish completely at 873 K and at 1173 K due to the formation of Sn–O–Bi bonds. There exist strong diffraction peaks of SnO_2 at calcination temperature of 873 K and 1173 K. As can be seen from Fig. 3, the specific diffraction peaks of (110), (101) and (211) sharpens when the calcination temperature increases from 573 K to 1173 K, which indicates that the crystal size tends to grow with increasing calcination temperature. The mean crystal sizes are 4.6, 5.8 and 15 nm when BTP is calcined for 3 h at 573, 873 and 1173 K, respectively.

Effect of PAM on the solid–liquid separation of colloidal precursor and particle size distribution of BTO powders

The characteristics and sharp of nano-BTO powders (calcined at 873 K) obtained after PAM treatment are shown in Table 1 and Fig. 5.

As can be seen from Table 1 and Fig. 5, the addition of PAM facilitates the formation of large flocs of BTP and reduces the filtration time. However, it is interesting to us

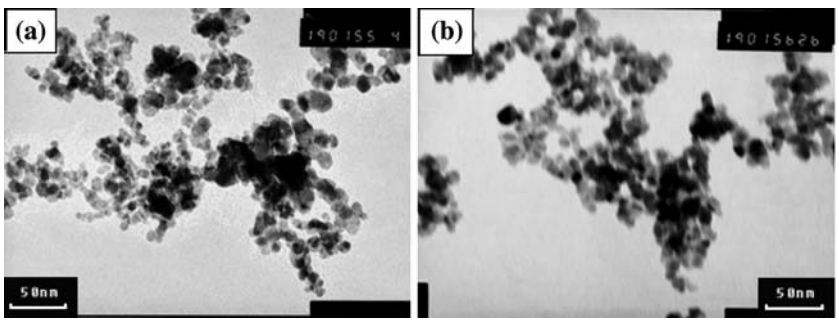

Fig. 4 TEM images of BTO powders prepared at 873 K (**a**) and 1173 K (**b**)

Table 1 Performances of PAM flocculants on BTP and BTO

Samples	PAM flocculants	Experimental phenomena	Filtration time/min	Average particle diameter of BTO, D (0.5)/nm
A	No addition of any flocculants	No flocs, no stratification	240	700
B	Anionic PAM ($M = 9 \times 10^6$)	Small flocs, slow deposition	82	43
C	Cationic PAM ($M = 1.2 \times 10^7$)	Large flocs, fast deposition	25	61
D	Nonionic PAM ($M = 1.2 \times 10^7$)	Large flocs, fast deposition	13	8

M: Molecule weight

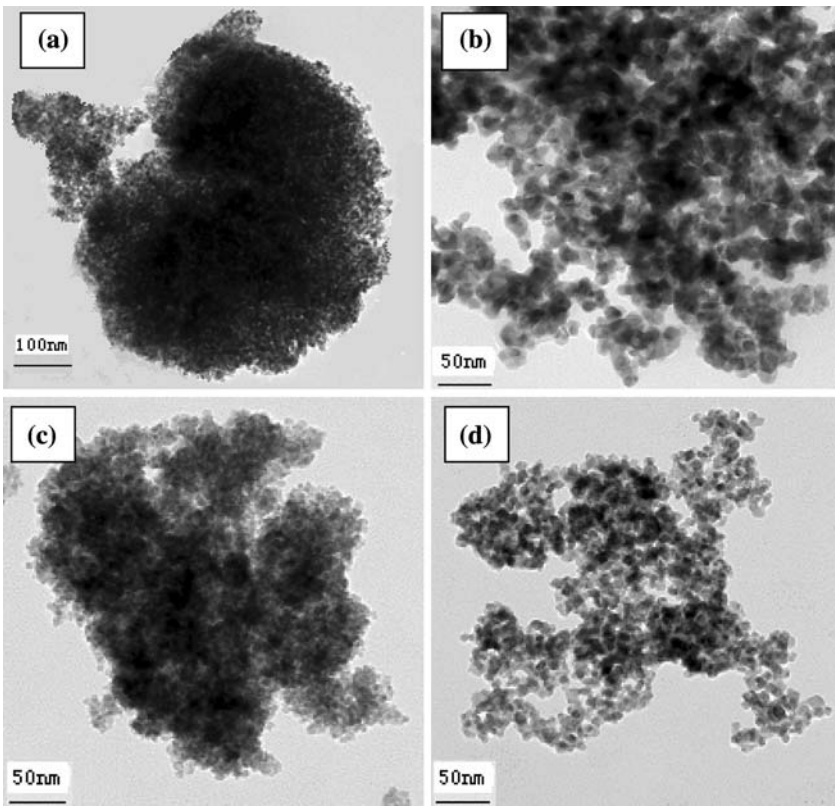

Fig. 5 Images of BTO when BTP was treated with different flocculants. (**a**) Without any flocculants; (**b**) anionic PAM; (**c**) cationic PAM; (**d**) non-ionic PAM

that the particle size of BTO does not increase with formation of large flocs, in contrast, the average particle size (d (0.5)) decreases mostly due to the application of PAM. The active hydroxyl groups and –O– bond exposed on the outside of BTP nanoparticles is occupied and encapsulated when BTP nanoparticles are adsorbed on the PAM molecule. The hard agglomerate of BTP nanoparticles is effectively prevented due to the steric hindrance of PAM molecule and the lack of active sites on BTP nanoparticles. In addition, the thermal decomposition of PAM and subsequent production of gases during calcination of BTP may be another reason that prevents the formation of hard agglomerates of particles. A great quantity of heat is carried out by the thermal decomposition of PAM, which prevents the occurrence of local overheating during the calcinations of BTP.

Among the three kinds of PAM used, nonionic PAM exhibits the best performance. Table 1 shows that the average particle diameter d (0.5) of BTO. 700 nm is without PAM, but it decreases to 43 nm, 61 nm and 8 nm if BTP was treated with anionic PAM, cationic PAM and nonionic PAM, respectively. Because the particles of BTP are negatively charged, the electrostatic repulsion between BTP nano-particles prevents the aggregation of BTP when it was treated with anionic PAM. The charge neutralization, bridging and adsorption of PAM caused fast formation of BTP flocs after the addition of cationic PAM. For nonionic PAM, it cannot absorb any other impure ions which effect hard agglomerates during the subsequent calcination, so, the particle size of BTO treated by nonionic PAM is smaller than that treated by cationic PAM and anionic PAM.

Conclusions

BTO nanopowders were prepared by wet chemical co-precipitation method using nonionic PAM as filtration aid and disperser. The average size of BTO is smaller than 10 nm. The optimal calcination temperature of BTP is about 873 K. Nonionic PAM is a highly effective aid in the preparation of BTO nanosized material, which not only speeds up filtration of BTP, but also effectively prevents the formation of hard agglomerates of BTO.

Acknowledgment The work was financially supported by the open fund of Guangdong provincial key laboratory for green chemicals (Granted No. GC200603).

References

1. Gorley PM, Khomyak VV, Bilichuk SV, Orletsky IG, Horley PP, Grechko VO (2005) Mater Sci Eng B: Solid 118(1–3):160
2. Calestani D, Zappettini A, Lazzarini L (2005) Mater Sci Eng C 25(5–8):625

3. Cássia-Santos MR, Sousa VC, Oliveira MM, Sensato FR, Bacelar WK, Gomes JW, Longo E, Leite ER, Varela JA (2005) Mater Chem Phys 90(1):1
4. He Q, Tu W, Hu J (2005) Chem Indus Eng Progress (Chin.) 14(10):1108
5. Tan J, Shen L, Fu X, Hou W, Chen X (2004) Dyes Pigment 6(1):31
6. Niesen TP, De Guire MR (2002) Solid State Ionics 151(1–4):61
7. Leite ER, Weber IT, Longo E, Varela JA (2000) Adv Mater 12(13):965
8. Aukkaravittayapun S, Wongtida N, Kasecwatin T, Charojrochkul S, Unnanon K, Chindaudom P (2006) Thin Solid Films 496(1):117
9. Han JB, Zhou HJ, Wang QQ (2006) Mater Lett 60(2):252
10. Miao HY, Ding CS, Luo HJ (2003) Microelectron Eng 66:142
11. Tan OK, Cao W, Hua Y, Zhu W (2004) Solid State Ionics 172:309
12. Li W, Zhou KC, Yang H (2004) J Mater Sci Eng (Chin) 22(1):154
13. Malinovskaya TD, Aparnev AI (2001) Russ J Appl Chem 74(11):1864
14. Rose-Noelle V, Edouard C, Caroline P, Cesar S, Guy N, Gaetan M, Chater RJ, Skinner SJ, Kilner JA (2003) Mater Res Soc 756:95